Soil & Tillage Research 234 (2023) 105844

Contents lists available at ScienceDirect

Soil & Tillage Research

journal homepage: www.elsevier.com/locate/still

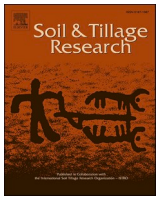

Prediction of the distribution of soil properties in deep Colluvisols in different pedogeographic regions (Czech Republic) using diffuse reflectance infrared spectroscopy

Lenka Pavlů [a,*], Tereza Zádorová [a], Jiří Pavlů [b], Václav Tejnecký [a], Ondřej Drábek [a], Jessica Reyes Rojas [a], Saven Thai [a], Vít Penížek [a]

[a] Czech University of Life Sciences Prague, Department of Soil Science and Soil Protection, Kamýcká 129, CZ-16500 Prague Suchdol, Czech Republic
[b] Charles University, Faculty of Mathematics and Physics, Department of Surface and Plasma Science, Ke Karlovu 3, CZ-12116 Prague 2, Czech Republic

ARTICLE INFO

Keywords:
Colluvial soils
Soil erosion
DRIFT spectroscopy
Spectra normalization
Organic matter quality

ABSTRACT

Colluvisols form a significant part of the erosion–deposition soil catena mainly in undulating, agriculturally managed landscapes. Due to their sedimentary origin, they are soils with highly variable properties. For such diverse and often extremely deep soils, it is essential to capture the vertical distribution of properties in as much detail as possible. This study demonstrates the potential of the diffuse reflectance infrared spectroscopy (DRIFT) to derive accurate information on the stratigraphy and selected soil properties (soil organic carbon and calcium carbonate contents and aluminium and iron concentrations) of deep colluvial profiles in three regions in the Czech Republic with different dominant soil types (Chernozem, Luvisol, and Cambisol). The normalization of the spectrum using the quartz spectral band was found to be suitable for assessing the carbonate content in Chernozems and Luvisols (coefficients of determination (R^2) were 0.89 and 0.88, respectively). The amount of organic carbon can be predicted from such normalized spectra with less confidence ($R^2 = 0.64$). Organic matter quality as an indicator of their stability and maturity was computed from aliphatic compounds spectral bands (2930 cm^{-1}) and aromatics and C=O groups band around 1640 cm^{-1}. The highest values of this indicator were found in Colluvisols in the Chernozem region (> 6, while, e.g., in the Cambisol region it is < 1), especially in the layers corresponding to the oldest sediments or buried in-situ horizons. In the Cambisol region, the buried B horizon was identified based on normalized (i) clays and Fe oxides bands and (ii) wider band of OH groups, which in this case is related to the content of iron oxyhydroxides. The study proved that the applied set of spectral parameters is an effective tool for the description of diverse soil parameters and for identification of the boundaries of individual soil layers. It is equally suitable for carbonate-free soils as well as for soils with higher carbonate contents, which usually cause difficulties in the interpretation of soil organic matter spectral parameters. It provides a comprehensive view of the soil and its mineral and organic components and can provide information that is difficult to measure by other methods.

1. Introduction

Colluvisols are a specific soil type arising at the foot of slopes or side valleys due to the sedimentation of eroded material transported from the wider area. They are a record of climatic fluctuations, changes in land use and varying soil tillage (Leopold and Völkel, 2007). Colluvisol formation varies between the sedimentation of relatively thick layers during intensive rainfall episodes and the slow accumulation of thin layers in drier periods (Zádorová and Penížek, 2018). The most commonly considered factors affecting the erosion intensity and formation of colluvial soils include: (i) transformation of forested areas and grasslands to agricultural land, enhancing soil redistribution through both the acceleration of surface runoff due to the removal of the stable vegetation cover and the disturbance of the soil balance, in particular the deterioration of the soil structure, leading to a higher susceptibility of the soil to erosion removal (Boardman and Poesen, 2006), (ii) landscape defragmentation, leading to the establishment of large homogeneous agricultural blocks and, conversely, the disappearance of natural

* Corresponding author.
E-mail address: pavlu@af.czu.cz (L. Pavlů).

https://doi.org/10.1016/j.still.2023.105844
Received 5 January 2023; Received in revised form 14 July 2023; Accepted 19 July 2023
Available online 27 July 2023

or artificial features acting as a barrier to translocated soil material, slowing down the surface runoff and retaining the surplus of water and material on the field (Foucher et al., 2014), (iii) intensive agriculture with use of heavy machinery and deeper, often up- and downslope, ploughing (Van Oost et al., 2006), causing displacement of material, i.e. tillage erosion, disturbance of soil aggregates and soil compaction, increasing the susceptibility to material removal during rainfall episodes, and (iv) crop rotation with long periods of bare soils, often leaving the land without vegetation cover during critical spring periods with increased occurrence of heavy rainfall events (Keesstra et al. (2016)). Decreasing tillage depth and ploughing along the contour lines, management of plant residues, intercrops and winter crops or grass margins are considered as feasible methods to reduce the intensity of soil material redistribution due to soil erosion (Van Oost et al., 2006; Kincl et al., 2022). The Czech landscape has undergone extreme changes in the last 70 years, related to the politically motivated collectivisation of agricultural production and the massive consolidation of agricultural land (Sklenička et al., 2014). The disappearance of landscape elements, the use of heavy machinery and the increase in the field size, together with undulating relief and vulnerable soils, led to intensive material redistribution not only in the most exposed loess areas (Sarapatka et al. (2018)), but also in the hilly regions with magmatic or metamorphic bedrock dominating in the Czech Republic (Zádorová et al., 2023). Colluvisols can reach considerable thicknesses and act as soil organic carbon reservoirs (Chaopricha and Marín-Spiotta, 2014; Zádorová et al., 2015). They can help to understand the causes and consequences of actual and past soil erosion, and they attract more attention as a key to our understanding of the landscape dynamics in the changing climatic conditions (Dotterweich, 2008).

To date, Colluvisols have been studied by a complex of different methods and approaches, revealing different aspects of their formation and post-depositional pedogenesis, first predominantly in loess regions (e.g., Zádorová et al., 2013; Kühn et al., 2017; Kołodyńska-Gawrysiak et al., 2018; Sherer et al., 2021a), more recently also in areas built on a wide range of non-loessic parent materials (Henkner et al., 2018; Kappler et al., 2018; Kaiser et al., 2020; Scherer et al., 2021b; Zádorová et al., 2023). Attention is paid mainly to the assessment of the age of individual layers. Optically stimulated luminescence (OSL), often in combination with the radiocarbon method, has been widely used for the datation (e.g., Fuchs and Lang, 2009; Poręba et al., 2015). Determination of radionuclide activity (^{137}Cs, ^{210}Pb, ^{10}Be, $^{239+240}$Pu) and human-bound vertically stable substances, such as organic pollutants (e.g., DDX, HCB), potentially risk elements or nutrients, can also be effectively used to assess both recent and long-term deposition (e.g., Clemens and Stahr, 1994; Zádorová et al., 2013; Poręba et al., 2019; Loba et al., 2022). The potential of their use is related to their affinity to soil components, mainly soil organic matter and clay, and thus a relatively low vertical mobility in the soil profile (van der Perk, 2006). Since for many substances the period of beginning or cessations of their use or input into the soil is known, it is possible to relate the increased concentrations of substances in a particular layer to a specific period of deposition (Zádorová et al., 2023). At the same time, the sedimentary soils provide an important record of the intensity of use of these compounds, including an understanding of the leaching process and residence time in the profile, which are essential for taking practical measures in soil management. The study of a wide range of chemical and physical parameters (Zádorová et al., 2013; Jakšík et al., 2015; Scherer et al., 2021a; Pavlů et al., 2022), soil micromorphology (e.g., Kühn et al., 2017), mineralogy (e.g., Dreibrodt et al., 2013, Zádorová et al., 2023) and microbial properties (e.g., Sagová-Marečková et al., 2016) can elucidate and describe a variety of depositional and pedogenetic processes alternating during the formation of these soils. However, most of these analyses are quite demanding in terms of time and instrumentation.

There are also less laborious indirect techniques using various types of sensors to identify elements or minerals in the soil profile, and organic matter content. Often used are portable X-ray fluorescence spectrometry and visible and near-infrared spectroscopy (Stockmann et al., 2016; Benedet et al., 2022; Gozukara et al., 2022) in studies focusing on soil profile differentiation.

Infrared (IR) spectroscopy in the middle infrared part of spectra (wavelength 2.5–25 μm; 4000–400 cm^{-1} respectively) is frequently used for the identification of pure chemicals. Part of the spectral range referred to as fingerprint (1500–400 cm^{-1}) is specific for different functional groups vibration in molecules. It depicts relatively sharp and well-identified peaks of specific spectral bands (Stuart, 2004). A more complicated situation is with spectra of mixtures where bands of individual functional groups overlap. Soil is a typical mixture containing a wide range of mineral and organic components. Thus, wider bands appear in the spectra (Haberhauer et al., 1998; Madejová, 2003; Leue et al., 2010; Le Guillou et al., 2015; Tinti et al., 2015) and the identification of individual substances is thus considerably limited. For example, OH group vibration in the range 3440–3320 cm^{-1} can belong to organic matter components or to minerals of group oxide–hydroxides. Spectral peak around 1520 cm^{-1} can belong to the C=C vibration of benzene rings together with the amid II functional group. Cunha et al. (2009) use this band for the calculation of index describing the aromatic components proportion in organic matter, while Haberhauer et al. (1998) uses it as an indicator of the decomposition of organic matter depending on the content of its nitrogenous components. Moreover, in the case of soil formed on carbonates substrates, this peak is entirely covered by a broad and intensive carbonates band. One of the approaches to analyse IR spectra is the evaluation of spectra as a whole and obtaining information with advanced mathematical operations (e.g., Ng et al., 2019). Partial least squares regression is the most common chemometric method used in the prediction of soil properties from diffuse infrared reflectance spectra (Minasny and McBratney, 2008). Other alternatives for spectral data processing and modelling can be using robust artificial intelligence approaches to solve problems exhibiting complex mechanisms, particularly in geoenvironmental engineering (Jalal et al., 2021) if a large data set is available for training the models. The second approach is, despite aforementioned difficulties, to select well-defined bands and used them specifically, e.g., for minerals identification (Senthil Kumar and Rajkumar, 2014; Bosch-Reig et al., 2017; Hahn et al., 2018), for determination of soil aggregates wettability which determines water behaviour in soils (infiltration, retention) (Ellerbrock et al., 2005; Leue et al., 2010; Thai et al., 2022), or for the evaluation of qualitative parameters of soil organic matter (Gerzabek et al., 2006; Pärnpuu et al., 2022). Various types of indexes were designed to evaluate SOM aromaticity (Cunha et al., 2009; Matamala et al., 2017) or level of decomposition (Haberhauer et al., 1998; Artz et al., 2006; Matamala et al., 2017).

Presented study aims to provide an alternative to the aforementioned direct and indirect methods. It aims to introduce the applicability of infrared spectroscopy in the middle infrared part of spectra (especially diffuse reflectance infrared spectroscopy with Fourier transformation (DRIFT)) as a rapid technic with relatively simple sample preparation providing a wide range of information on soil properties applicable at complex Colluvisols description. The main effort of this paper was to propose spectral indicators usable with the same reliability for both carbonate and non-carbonate soils and to test their effectiveness in the identification of horizons of very deep colluvial soils varying in mineralogical properties, organic carbon content, and organic matter quality. This study aims to introduce an original set of relatively easy measured soil spectral parameters not requiring advanced mathematical processing or large datasets which can describe soil chemical properties, (i) qualitative (identification of the presence of certain minerals or relative comparison of the representation of different organic matter components using only spectral bands nonoverlapping with carbonate bands) and (ii) quantitative (evaluation of the amount of organic matter or carbonates in the soil using the spectra normalization by the quartz spectral band) both on the example of Colluvisols (three regions with

different lithology, climatic conditions and soil types) and (iii) determine their usefulness for defining the individual Colluvisols layers the subsequent detailed investigation of which can disentangling the complex functioning and formation history of colluvial soils.

2. Methods

2.1. Sites description

Three localities (Brumovice, Vidim, and Kosova Hora; Fig. 1) fundamentally different in their geological and pedological conditions, climate and settlement history but with similar topography were selected for this study. The naming of soil types and subtypes presented below is based on the classification (IUSS Working Group WRB, 2022).

Brumovice is situated in a loess region in South Moravia in the Czech Republic. The average annual temperature varies between 9 and 10 °C, and the average annual precipitation is between 500 and 550 mm. The history of this site and Colluvisols forming conditions are described by Zádorová et al., (2013, 2023). Soil cover is created on a Pleistocene loess layer with a variable depth ranging from several meters up to several tens of meters (Chlupáč et al., 2002). Calcic Chernozem is the original dominant soil unit in the region, which is now gradually transforming into different soil units as a result of intensive erosion and redeposition of soil material (Jakšík et al., 2015). Areas with minimal slope (0–2°) are covered mainly by Calcic Chernozems, areas with increasing slope by its eroded forms, and the steepest parts (8–15°) of the slopes by Regosols and Calcisols. Loess itself is exposed in many cases. Colluvial soils (Kastanozems and Phaeozems (Solimovic) with deep humus horizons are formed in slope depressions (Zádorová et al., 2013). The research was performed on an agricultural parcel (area of 6 ha), forming a complex slope system with different landforms.

Vidim is situated in Central Bohemia (Czech Republic), in the Pšovka River watershed. The wider area is underlain by Cretaceous sandstones covered by a Pleistocene loess layer (Chlupáč et al., 2002). Haplic and Albic Luvisols are the original dominant soil units. The average annual temperature varies between 7 and 8 °C, and the average annual precipitation is between 550 and 650 mm. The study plot (4.5 ha of agricultural soil) is characterized by intensive topography dominated by two side valleys connected in the southwest part of the site. These two concave units represent the main accumulation positions at the plot, where colluvial soils (Haplic Luvisols (Solimovic) developed. The adjacent slopes, covered by eroded Luvisols and Regosols, are relatively

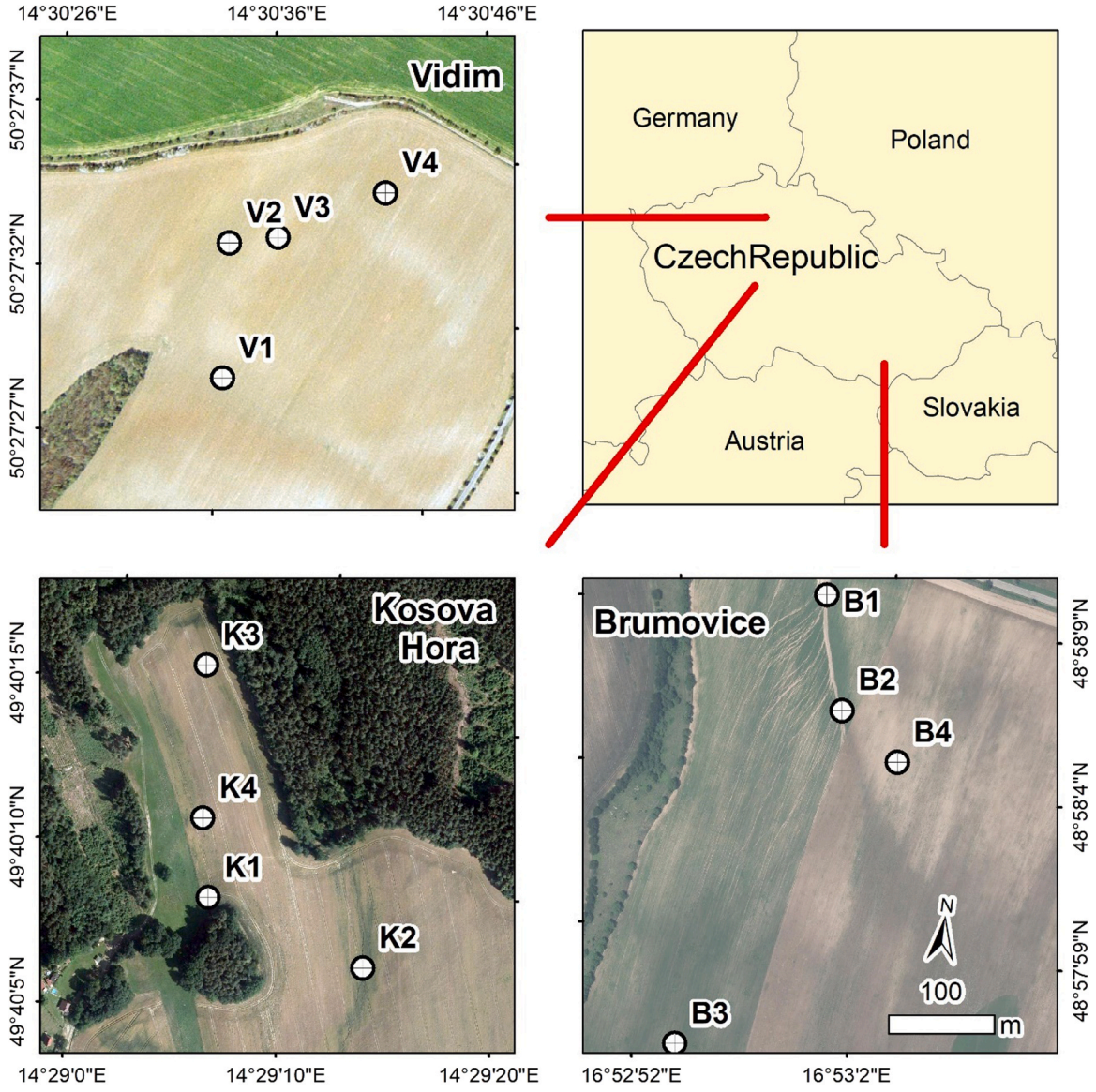

Fig. 1. Studied localities and soil pit positions.

steep (up to 12°), while the plot's south, northeast, and northwest parts are formed by flat terrain. More details about this site are given in Zádorová et al. (2014), Penížek et al. (2016), and Pavlů et al. (2022).

Kosova Hora is situated in the central part of the Czech Republic in the Central Bohemian Upland. Geologically, the area forms part of Central Bohemian magmatic pluton. The parent material of the study area derives from granodiorites, in the side valleys covered by silty deluvial sediments (Chlupáč et al., 2002). The average annual temperature varies between 7 and 8 °C and annual precipitation is between 600 and 700 mm. The study plot covers an area of 10 ha of agricultural soil. The terrain is complex comprising of backslopes, a side valley, and two significant colluvial–alluvial cones at the toe-slopes. Eutric Cambisols are the dominant soil units, significantly eroded at the slopes. Zádorová et al. (2023) described occurrence of Luvisols at the study area, namely in the flat parts of the terrain. Skeletic Leptosols occur at the steepest parts. Stratified Colluvisols (Solimovic Cambisols) developed in concave positions.

2.2. Soil sampling

Soil samples were collected from four soil pits in each area (Table 1). One pit always captures soil negligibly affected by erosion in the higher and flatter parts of the area. The second was dug in the most eroded sloping part of the area. The remaining two were located in places of accumulation of eroded material (toe-slope and side valley). Soil samples were taken every 10 cm down to the depth of the original soil-forming substrate or in-situ soil material. They were air-dried, ground, and sieved through a 2-mm sieve to analyse selected soil properties. The soil samples were ground to analytical fineness to measure the infrared spectra. For the detailed description of the field survey and selection of sampling points see Zádorová et al. (2023).

2.3. Soil chemical analyses

Soil organic carbon (SOC) content was measured using the dichromate redox titration method (Skjemstad and Baldock, 2007). $CaCO_3$ content was measured using the volumetric method corresponding to the ISO 10693 standard (08.53 calcimeter – Ejkelkamp).

Element contents (Fe_{AR}, Al_{AR}) in aqua regia extract were measured using the method of Cools and De Vos (2016). The final concentrations of Fe and Al were subsequently measured by inductively coupled plasma–optical emission spectrometry (ICP–OES) using an iCAP 7000 radial ICP emission spectrometer (Thermo Fisher Scientific Inc., USA) under standard analytical conditions.

2.4. DRIFT spectra measurement and description

MID infrared spectra were measured using the diffuse reflection technique and instrument Nicolet iS10 (Thermo Fisher Scientific Inc., USA). The spectral range was 4000–400 cm^{-1}. Before the measurement, the samples were not diluted with KBr or otherwise modified. The gold mirror was used as a background reference. The 64 scans with a resolution of 4 cm^{-1} and spectra conversion to Kubelka–Munk units were applied. OMNIC 9.2.41 software (Thermo Fisher Scientific Inc., USA) was used for spectra analysis. Well-definable bands of soil components functional groups were determined in the spectra and their reflectance converted to Kubelka–Munk units was measured.

Fig. 2 shows average DRIFT spectra of soils in all three studied regions. Description of main spectral bands of soil presents Table 2. Most of the listed spectral bands of both mineral and organic soil components can be found in all soil types. The exception are the bands of carbonates (around 2515 cm^{-1} and 1450 cm^{-1}) which are visible in the spectra only when their content is higher in the soil (approximately > 1 %). Unfortunately, the intensive band in the 1450 cm^{-1} overlaps the bands of some functional groups (1545–1500; aromatic C═C stretching, aromatic skeletal vibration, aromatic (lignin), amide II) suitable for a

Table 1
Soil profiles description and accumulation period of individual layers based on Zádorová et al. (2023).

Brumovice	Layer / horizon	Depth (cm)	Period of accumulation
B1	Ap	0–25	last 30 years
Solimovic Regosol (Protocalcic, Siltic) over Calcic Chernozem	M1	25–100	last 70 years
	M2	100–150	Middle Ages
	M3	150–220	Middle Ages
	M4	220–270	Dark Ages
	M5	270–300	Late Neolithic
	2Ahb	300–350	
	2AC	350–370	
	3Ck	370–380	
B2	Ap	0–27	
Haplic Kastanozem (Siltic, Solimovic) over Calcic Chernozem (Stagnic)	M1	27–70	Middle Ages
	M2	70–120	La Tene period
	M3g	120–170	Middle Bronze Age
	M4	170–190	Early Bronze Age
	M5	190–250	Early Holocene
	2Ahgb	250–300	
	2Bwg	300–340	
	3Ckg	340–350	
B3	Ap	0–25	
Calcic Chernozem (Siltic)	Ah	25–40	
	AC	40–50	
	Ck	50–70	
B4	Ap	0–25	
Haplic Calcisol (Siltic)	Ck	25–60	
Vidim	**Layer / horizon**	**Depth (cm)**	**Period of accumulation**
V1	Ap	0–30	
Haplic Luvisol (Siltic, Cutanic, Solimovic)	M1	30–75	Late Middle Ages
	M2	75–112	Early Middle Ages
	M3	112–123	
	M4	123–160	Roman period
	M5	160–185	Roman period
	2Ahb	185–205	
	2Egb	205–220	
	2Btgb	220–240	
V2	Ap	0–30	
Haplic Luvisol (Siltic, Cutanic, Solimovic)	M1	30–55	Middle Ages
	M2	55–80	
	M3	80–92	Middle Ages
	M4	92–110	
	M5	110–170	Early Middle ages/ Dark Ages
	M6g	170–200	Early Middle ages/ Dark Ages
	2Btgb	200–220	
V3	Ap	0–37	
Calcic Luvisol (Siltic, Cutanic)	Bt	37–73	
	Bt/C	73–95	
	Ck	95–120	
V4	Ap	0–34	
Calcaric Regosol (Siltic)	C	34–80	
Kosova Hora	Layer/ horizon	Depth (cm)	Period of accumulation
K1	Ap	0–20	last 30 years
Eutric Solimovic Bathystagnic Regosol (Loamic)	M1	20–32	last 30 years
	M2	32–40	last 30 years
	M3	40–57	last 70 years
	M4	57–70	last 70 years
	M5	70–90	last 70 years
	M6	90–107	Middle Ages
	2Bg	107–120	
	3Bg	120–137	Early Holocene
	4Bg	137–180	
K2	Apg	0–27	
Eutric Solimovic Stagnic Regosol (Loamic)	M1g	27–160	Middle Ages
	M2g	160–180	Early Middle ages/ Dark Ages
K3	Ap	0–26	
Haplic Luvisol (Loamic)	Btw	26–63	
	C	63–80	
K4	Ap	0–25	
Eutric Lithic Leptosol	C	20–40	

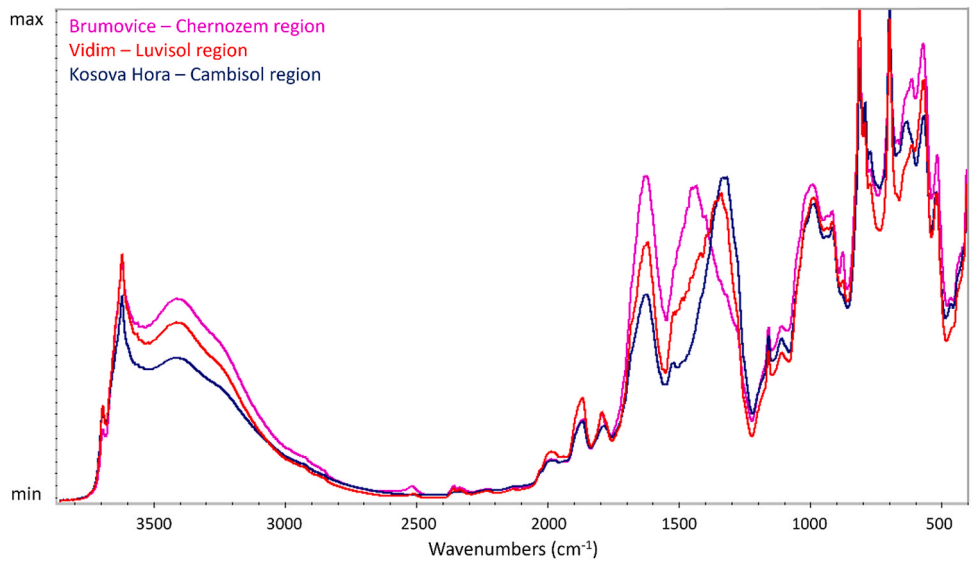

Fig. 2. Average DRIFT spectra of soils from three studied regions in full-scale (min–max) display.

Table 2
The assignment of the major spectral bands in the soil infrared spectra (Haberhauer et al., 1998; Madejová, 2003; Vagenas et al., 2003; Leue et al., 2010; Le Guillou et al., 2015; Tinti et al., 2015).

Spectral band (cm^{-1})	Description
3700–3680	Si–O–H vibration of clays and Fe oxides (weak hydrogen bonds with the oxygens of the Si–O–Si bonds on the lower surface of the next layer)
3630–3620	Si–O–H bonds in clays and oxides (hydroxyl groups, lying between the tetrahedral and octahedral sheets)
3440–3320	O–H and H–bonded OH (mainly in organic components – alcohols, carboxyl functions, phenols)
3010–2800	aliphatic $–CH_2$ and $–CH_3$ stretching
2550–2500	carbonates
2000–1790	Si–O vibration of quartz (and 1800 calcite) overtone
1775–1711	C═O stretching in carboxylic group
1690–1570	C═O stretching of amides (amide I), H–bonded conjugated ketones, carboxyls and quinones, C═N stretching, amide II of primary amides, aromatic C═C
1545–1500	aromatic C═C stretching, aromatic skeletal vibration, aromatic (lignin), amide II
1470–1420	carbonates
1430–1300	aliphatic C–H deformation of CH_2 and CH_3 bending, C–OH deformation of COOH, C═O, and C–O stretching of phenolic groups, COO– and O–H
1160	O–Si–O in quartz
1100–1050	polysaccharides
1030–1000	Si–O of silicate stretching in feldspars and secondary alumosilicates
810 and 780	quartz doublet
695	quartz

qualitative description of the composition of soil organic matter according to, e.g., Haberhauer et al. (1998) or Cunha et al. (2009). In such cases, either a more complex preparation of the samples or mathematic peak resolve (both of which can introduce an error into the result) is necessary.

In this study, a ratio of the band around 1640 cm^{-1} and the aliphatic band (around 2930 cm^{-1}) was designed and used as an indicator describing organic matter quality (OMQ). These two spectral bands were used because they do not overlap even in carbonate soils and identify important components of SOM. Based on their ratio, the relative proportion of aliphatic, aromatic, or C═O-containing groups of SOM can be evaluated.

2.5. Normalization of the DRIFT spectra

In order to quantify the selected spectral parameters, the non-quantitative DRIFT spectra must be adjusted or normalized. Calculation of peak relative absorbances are often used. They were calculated by dividing the distinct peaks heights by the sum of the heights of all peaks and multiplying it by 100 (Gerzabek et al., 2006). In this case, we chose a different approach based more on the basic principle of soil formation. Quartz is one of the most stable minerals in the soil, and also precisely because of this, it belongs to the most abundant minerals in most soil types (Brady and Weil, 2008). The DRIFT spectrum shows the quartz bands at 1160 cm^{-1}, well-defined sharp doublet at 810 and 780 cm^{-1}, and the band at 695 cm^{-1} (Le Guillou et al., 2015). Bands of quartz are some of the most intense in the spectra of soils. They are narrow and do not overlap with others. For that reason, they were used for normalization. The spectra were normalized with the reflectance (converted to Kubelka–Munk units) of the bands at 695 cm^{-1} and 810 cm^{-1}, respectively. Both normalizations were compared. Fig. 3 shows that both normalizations return similar but not the same results. The best matches are reached in the carbonate band (2520 cm^{-1}). The

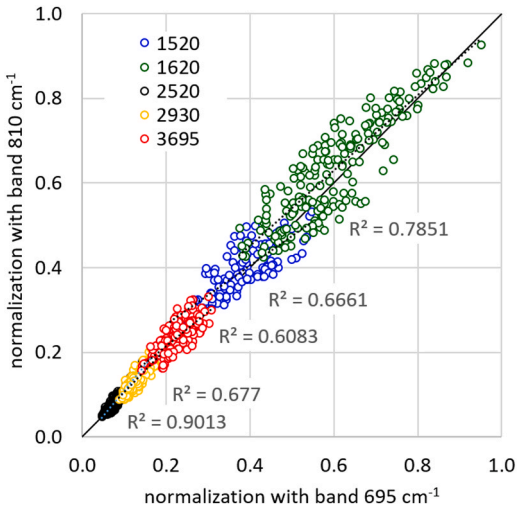

Fig. 3. Comparing of two types of spectra normalization. Coefficients of determination (R^2) was computed separately for selected spectral bands. Black full line indicates theoretical 1:1 relationship.

selection of a more appropriate type of normalization was therefore further tested using basic soil properties.

The heights of peaks in the normalized spectra were correlated with the soil parameters measured by standard analytical methods (Table 3). STATISTICA 13.3 software (StatSoft Inc., USA) was used to perform correlation analysis. The heights of spectral peaks, whose shapes and intensities were not affected by the presence of carbonates, were included in the correlation analysis for all samples (N 195). The values affected by the presence of carbonates were excluded from the analysis (N 120), therefore, the correlation coefficients in such cases are valid only for samples with zero or very low carbonate content. Table 3 documents that better results (higher correlation coefficients) can be achieved when normalizing with the 810 cm^{-1} band.

3. Results and Discussions

3.1. Using DRIFT normalized spectra as soil chemical parameters predictors

In addition to the more appropriate type of normalization, the correlation analysis also indicated which soil parameters can be derived on the base of normalized spectra. SOC content correlate significantly with all spectral parameters belonging SOM (2925, 2850, 1620, and 1512 cm^{-1}). The highest correlation was found for SOC and sum of all SOM peaks heights. The disadvantage of this spectral parameter is its unsuitability for carbonate soils, where two (2850 and 1512 cm^{-1}) of the four bands used are deformed or covered by a band of carbonates. With regard to all types of soil, it appears to be the most suitable band of organic substances (1620 cm^{-1}).

Carbonates appear in two bands in IR spectra (around 2515 cm^{-1} and 1450 cm^{-1}). The first of these is well isolated from the other bands and, although it is less intense than the second mentioned, is well identifiable and measurable. The 1450 cm^{-1} band is located in the fingerprint area, it is very intense, but as an easy usable parameter it is unsuitable due to the number of overlaps. Very high correlation was found for $CaCO_3$ content and 2515 cm^{-1} peaks heights.

Two well defined peaks (3690 and 3620 cm^{-1}) belong, according to the literature (Madejová, 2003; Le Guillou et al., 2015; Tinti et al., 2015), to the vibration of clays (alumosilicates) and Fe oxides. Each peak individually correlates with aluminium and iron contents. However, higher correlation coefficients were achieved after summing the heights of both evaluated peaks.

The possibility of predicting soil parameter values from normalized DRIFT spectra was tested using simple regression analysis. Predictive models for estimating the SOC, $CaCO_3$, Al_{AR} and Fe_{AR} concentrations in soil separately for studied areas and soil regions was designed. The coefficients of determination (R^2), root mean squared error of prediction (RMSEP – the differences between predicted and observed values quantifying the accuracy of the prediction by comparing the prediction errors of different models), and residual prediction deviation (RPD – the standard deviation of observed values divided by the RMSEP) were calculated to verify the model quality (Table 4). The RPD considers both prediction error and variation in observed values, resulting in a model validity metric that is objective and easily comparable across model validation experiments (Williams and Sobering, 1993). The result shows that carbonate content in the Chernozem and Luvisol regions is the best-predicted soil property (high R^2 and low RMSEP; range of $CaCO_3$ content 0–25 %). A specific situation is in the Cambisol region where $CaCO_3$ concentrations are zero or very low (max = 0.07 %), resulting in low RMSEP but also very low R^2. The prediction of carbon concentration from FTIR spectra is well known (Barra et al., 2021) and the larger and more diverse the dataset, the more accurate is the prediction. In this case, we are working with a limited dataset with relatively low variability in organic carbon content (min = 0.06 %; max = 1.90 %). Accordingly, the organic carbon content is better predictable if data from all regions are used, although there is often less RMSEP and RPD in models from individual regions. Better results were obtained using more spectral bands of soil organic components. In this case, samples with a higher carbonate content had to be excluded from the calculations, as some of their bands overlap bands of organic soil components, as mentioned above. Predictions of Al_{AR} and Fe_{AR} contents are the most accurate (highest R^2 and lowest RMSEP) for the Luvisol region. However, even there their coefficients of determination are relatively low.

3.2. Application of normalized DRIFT spectra in Colluvisols description

From the results published also by Zádorová et al. (2023) and used there for comparison with spectral parameters (Figs. 4–6) it is evident that SOC concentrations are very low in soils of all these localities. SOC content is only higher in the Chernozem region – Brumovice (maximal values of SOC content: 1.8 % in the oldest sediments, 1.5 % in the Ap horizon, respectively) than in others (Vidim – Ap – 1.2 %; Kosova Hora – Ap – 1.1 %). Cambisol region differs from others in higher content of Al_{AR} and Fe_{AR} as elements abundant mainly in B horizons and in their almost zero carbonate content, unlike soils formed on loess (Chernozem and Luvisol region), where in some layers carbonate content reaches up

Table 3
Correlation coefficients identifying relationships among basic soil characteristics and spectral bands (computed normalized band height or sum of these heights; Σalif – sum of 2925 and 2850 band heights; Σorg – sum of 2925, 2850, 1620, and 1512 band heights; Σclay – sum of 3690 and 3620 band heights).

Band (s)	NB_{3690}	NB_{3620}	NB_{2925}	NB_{2850}	NB_{2515}	NB_{1620}	NB_{1512}	Σalif	Σorg	Σclay
N	195	195	195	120	195	195	120	120	120	195
	normalization with band 695 cm^{-1}									
SOC	−0.265 * **	0.260 * **	0.578 * **	0.476 * **	−0.064	0.711 * **	0.440 * **	0.551 * **	0.701 * **	0.112
$CaCO_3$	−0.406 * **	−0.127	0.072	0.178	0.850 * **	0.098	0.197 *	0.211 *	0.275 * *	−0.228 * *
Al_{AR}	0.332 * **	0.330 * **	−0.049	−0.014	−0.324 * **	−0.195 * *	−0.542 * **	0.008	−0.272 * *	0.359 * **
Fe_{AR}	0.294 * **	0.383 * **	−0.050	−0.047	−0.314 * **	−0.157	−0.525 * **	−0.019	−0.246 * *	0.387 * **
	normalization with band 810 cm^{-1}									
SOC	−0.252 * **	0.277 * **	0.485 * **	0.384 * **	−0.057	0.757 * **	0.611 * **	0.444 * **	0.801 * **	0.130
$CaCO_3$	−0.193 * *	0.113	0.273 * **	0.097	0.885 * **	0.315 * **	0.210 *	0.122	0.260 * *	0.023
Al_{AR}	0.532 * **	0.497 * **	0.088	0.214 *	−0.215 * *	−0.096	−0.386 * **	0.226 *	−0.041	0.558 * **
Fe_{AR}	0.441 * **	0.509 * **	0.050	0.127	−0.224 * *	−0.082	−0.426 * **	0.145	−0.071	0.537 * **

*, * *, * ** Significant at the probability level 0.05, 0.01, and 0.001, respectively; correlation coefficients of later discussed (3.1) relationships are in red.

Table 4
Linear regressions models and their coefficients of determination (R^2), root mean squared error of prediction (RMSEP), and residual prediction deviation (RPD). NB – normalized band height; Σorg – sum of 2925, 2850, 1620, and 1512 band heights; Σclay – sum of 3690 and 3620 band heights.

	N	regression equation	R^2	RMSEP	RPD
All sites	195	$SOC = 2.880(NB_{1620})^{* **} - 1.172^{* **}$	0.574	0.302	1.532
Chernozem region	85	$SOC = 3.370(NB_{1620})^{* **} - 1.540^{* **}$	0.368	0.354	1.258
Luvisol region	58	$SOC = 2.769(NB_{1620})^{* **} - 1.102^{* **}$	0.339	0.288	1.170
Cambisol region	46	$SOC = 2.056(NB_{1620})^{* **} - 0.751^{* *}$	0.272	0.212	1.171
all sites	120	$SOC = 2.000(\Sigma org)^{* **} - 1.818^{* **}$	0.641	0.319	1.669
Chernozem region	35	$SOC = 1.342(\Sigma org)^{* **} - 0.639$	0.441	0.262	1.451
Luvisol region	39	$SOC = 1.922(\Sigma org)^{* **} - 1.714^{* **}$	0.445	0.251	1.343
Cambisol region	46	$SOC = 0.842(\Sigma org)^{* **} - 0.655^{* *}$	0.322	0.204	1.214
All sites	195	$CaCO_3 = 168.8(NB_{2515})^{* **} - 11.28^{* **}$	0.787	2.276	2.155
Chernozem region	85	$CaCO_3 = 191.6\ (NB_{2515})^{* **} - 13.16^{* **}$	0.885	2.023	2.951
Luvisol region	58	$CaCO_3 = 166.2(NB_{2515})^{* **} - 9.892^{* **}$	0.876	1.323	2.706
Cambisol region	46	$CaCO_3 = -0.500(NB_{2515})^{*} + 0.066^{* **}$	0.099	0.041	0.498
Cher.+Luv. Regions	131	$CaCO_3 = 175.2(NB_{2515})^{* **} - 11.14^{* **}$	0.879	1.980	2.691
All sites	195	$Al_{AR} = 23892(\Sigma clay)^{* **} - 4187^{*}$	0.310	3837	1.205
Chernozem region	85	$Al_{AR} = 10898(\Sigma clay)^{* **} + 5139$	0.092	2467	1.050
Luvisol region	58	$Al_{AR} = 19531(\Sigma clay)^{* **} - 2224$	0.572	2345	1.455
Cambisol region	46	$Al_{AR} = 40453(\Sigma clay)^{* **} - 13662^{* *}$	0.493	5051	1.405
All sites	195	$Fe_{AR} = 21471(\Sigma clay)^{* **} + 1007$	0.289	3629	1.186
Chernozem region	85	$Fe_{AR} = 9641(\Sigma clay)^{*} + 9884^{* *}$	0.048	3101	1.025
Luvisol region	58	$Fe_{AR} = 18706(\Sigma clay)^{* **} + 2036$	0.550	2346	1.419
Cambisol region	46	$Fe_{AR} = 34012(\Sigma clay)^{* **} - 6684$	0.440	4727	1.337

* , * *, * ** Significant at the probability level 0.05, 0.01, and 0.001, respectively.

to 25 %.

Normalized spectra are presented as soil profile spectral maps (Figs. 4–6). These maps are supplemented with data of measured soil characteristics in the corresponding layers. The maps mainly show variability in the height/intensity of the normalized bands of OH groups (3440–3320 cm^{-1}), bands of organic substances (1690–1570 cm^{-1}), and bands of carbonates (1470–1420 cm^{-1}). This intensity corresponds very well with the measured soil properties. The z-axis scale is set so that the map best captures the variability of these intense bands. Less intense bands of aliphatic groups or carbonates in the region 2550–2500 cm^{-1} are therefore less visible. In general, it can be stated that this form of spectrum processing/visualization documents changes in soil properties along the depth gradient and can help in the identification and description of the individual layers of the Colluvisols discussed below.

In addition, spectra can also provide information on the qualitative parameters of soil organic matter, in this case, represented as OMQ index. Based on this ratio, the relative proportion of aliphatic, aromatic, or C═O-containing groups of SOM is evaluated. This proportion determines the mobility or stability of SOM through these components' affinity for soil minerals and for water. Aromatic compounds are less mobile, therefore, they are likely retained in the mineral soil horizon (Bi et al., 2013). Aromatic and aliphatic acids, such as for example lignin monomers, appear to be selectively retained on mineral surfaces and polysaccharides and protein appear to be selectively preserved in organo-metallic complexes (Angst et al., 2021). Absorption bands at 2921 and 2852 cm^{-1} indicate the hydrophobic (alifatic) groups of SOM and at the 1630 cm^{-1} hydrophilic groups (aromatic and C═O groups (O and N containing hydroxyl and carboxyl groups)). Aromatic rings, generally assumed to indicate hydrophobic groups, can show hydrophilic properties if they are conjugated with C═O groups (Ellerbrock et al., 2005; Leue et al., 2010). SOM richer in aromatic, alkyl, and carboxyl groups, but containing lower amounts of hetero-alkyl groups can be considered as more humified and chemically mature. Conversely, a lower number of aromatic groups and a higher percentage of O, N-alkyl C, predominantly in carbohydrate and polypeptide structures, represents a lower degree of humification and chemical maturity (Maryganova et al., 2010).

It has been shown, that aromaticity of organic matter increases in the common intact soil profiles with degrees of decomposition, maturity of OM and generally with depth (Veum et al., 2014; Margenot et al., 2015; Thai et al., 2021). The profiles of Colluvisols are specific and the quality of organic matter can vary depending on the sedimentation history of the layers and the origin of the sedimented material. Soil burial can isolate organic matter from the atmosphere, creating environmental conditions unfavorable to microbial decomposition, which can lead to the persistence of SOC relatively unchanged for thousands of years and conversely once exposed to ambient conditions, soil microbial activity can recover to rates comparable to surface soils (Chaopricha and Marín-Spiotta, 2014). And it is precisely this variability that the OMQ index can capture well.

In the Chernozem region (Fig. 4), the deepest Colluvisols were found with the aggregate thickness of colluvial layers exceeding 300, resp. 250 cm in the profiles B1 and B2. Buried profiles of former Chernozems were identified below the colluvial material (Zádorová et al., 2023). Chernozems are characterized by a thick very dark-coloured chernic surface horizon (Ah) passing into a light-coloured soil-forming substrate rich in carbonates (Ck) (IUSS Working Group WRB, 2022). Sharp change in $CaCO_3$ content between recent or buried Ah horizon and loess is evident in the B1 and B3 (less evident in the B2) spectral maps, both in the band 1470–1420 cm^{-1} and 2550–2500 cm^{-1}. The buried Ah horizons and oldest sedimented layer M5 in B1 profile and M3–5 in B2 profile are almost decalcified. Layers M4(B1) and M2(B2) are in spectral map defined by gradual transition and $CaCO_3$ content increase. In the spectral maps, medieval colluvial layers (B1 – M3 and M2) and recently deposited layers (B1, B2 – M1 and Ap) with high $CaCO_3$ content are well identified. These layers reflect accumulation of material transported from truncated source profiles, such as B4 (Zádorová et al., 2023) and represent a long-term erosion process and soil degradation in a landscape of south Moravia Chernozem region (Jakšík et al., 2015; Sarapatka et al., 2018).

Intensity of spectral band around 1620 cm^{-1} well describes the distribution of organic matter in soil profiles. Orange and red colours correspond to the buried Ah horizon and oldest sedimented layer M5 in B1 profile and to M5 and M4 layers in B2 profile. In the B1 profile the organic matter distribution is also reflected in broad band of OH vibrations in the range 3500–3300 cm^{-1}. The vibration of the OH group belongs mainly to organic components — alcohols, carboxyl, and phenols, as was mentioned in Table 1 (e.g., Tinti et al., 2015). Different situation is in B2 profile where this band is similarly intense in whole profile, including layers with very low SOM content. A wider band of OH groups in the case of these layers may correspond to higher contents of minerals belonging to (oxy)hydroxides (Madejová, 2003; Tinti et al.,

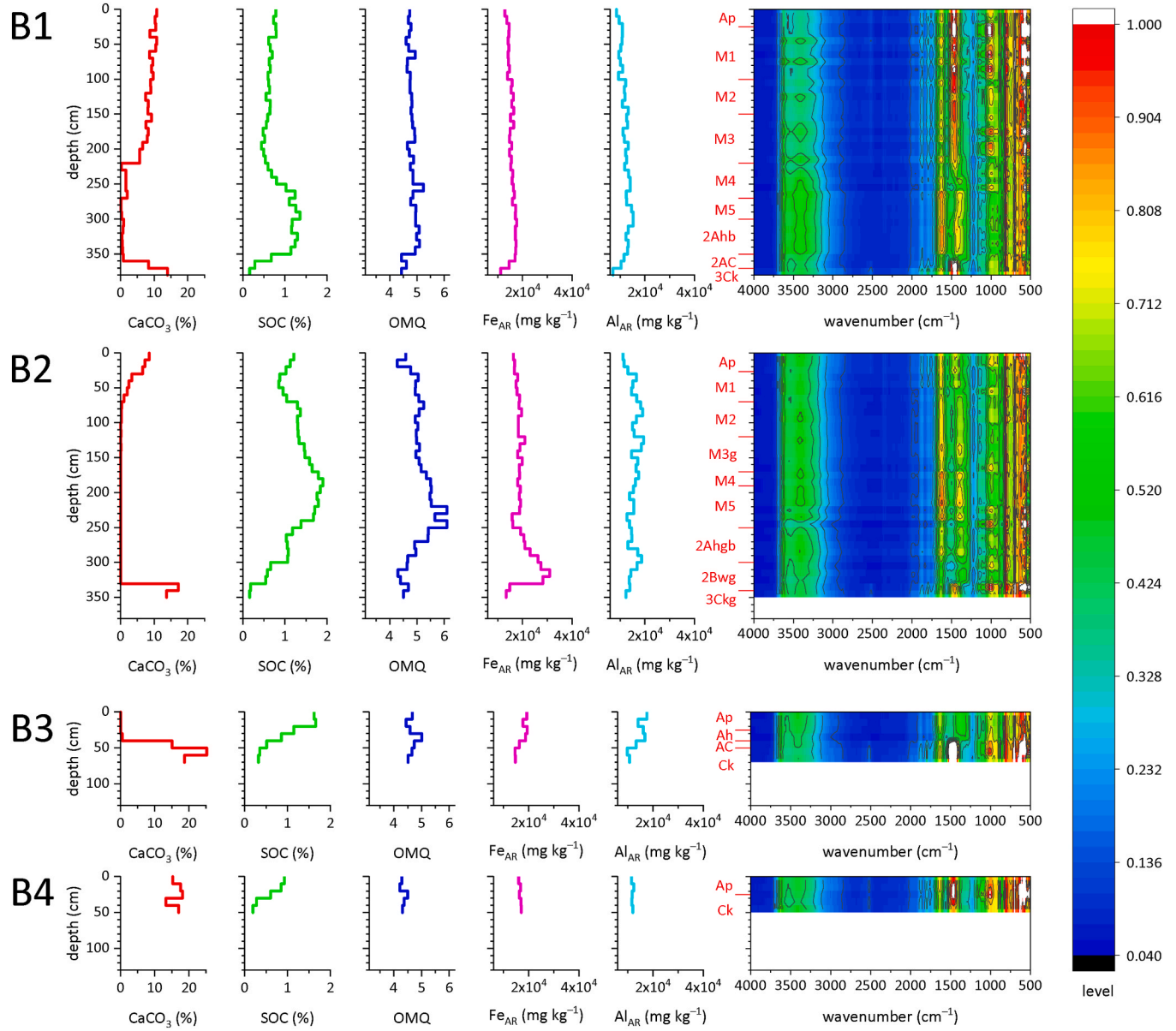

Fig. 4. Brumovice – Chernozem region – soil profiles distributions of $CaCO_3$ and SOC contents, organic matter quality (OMQ) index, Fe_{AR} and Al_{AR} contents, and spectral maps after spectra normalization by band 810 cm^{-1}.
Soil horizons description is adopted from Zádorová et al. (2023).

2015). Zádorová et al. (2023), who presented mineralogical composition of these soil profiles, identified the highest goethite (FeO(OH)) abundance in 2Bwg (B2) horizon. Also Fe_{AR} concentration in this horizon is higher than in other parts of B2 profile. Band of OH group is relatively intense there, but 1620 band of organic matter is weak. These two pieces of information together can therefore indicate the presence of OH groups in the mineral components of the soil. On the contrary, if the content of (oxy)hydroxides in the soil profile does not change (such as in B1), the band of OH groups can indicate the amount of organic matter.

Quality of organic matter is documented by OMQ index. The higher the ratio, the higher is the relative proportion of aromatic and C═O-containing groups of SOM (and relative proportion of aliphatic groups of SOM is lower). In general, the values of this index higher in the Chernozem region (compared mainly to the Cambisol regions) and the highest are in the Ah horizons or in oldest sediments. The highest values of this index were found in M5 layer of B2 horizon. Accumulation of this colluvial layer falls into the Early Holocene period (7940 ± 500 years BP) (Zádorová et al., 2023) and the deposition of exclusively humic material from the chernic horizons of the source soils is assumed. The organic matter with the lowest proportion of aliphatic components occurs at a depth of 230–250 cm. From this point of view, it can be characterized as stable and relatively recalcitrant and very resistant to decomposition (Maryganova et al., 2010; Bi et al., 2013; Angst et al., 2021). The values of this index are lower in the Ap horizons or recent sediments of all the studied profiles, which proves the presence of fresher, less stabilized organic matter richer in aliphatic components, e.g., polysaccharides, proteins, aliphatic organic acids, etc.

Like the previously discussed Chernozems, Luvisols also developed on loess but only after previous decalcification of the upper parts of the soil profile. Carbonates bands in ranges 1470–1420 cm^{-1} and 2550–2500 cm^{-1} are therefore the most obvious in Ck horizon of V3 profile. Furthermore, they are visible in profile V4, where confirmed difference between Ap (higher $CaCO_3$ content) and C horizon. The only band in range 1470–1420 cm^{-1} is partially displayed in V2 profile as extension band around 1300 cm^{-1}. This extension is evident from M3 layer to soil surface. Higher $CaCO_3$ contents appeared in the soil

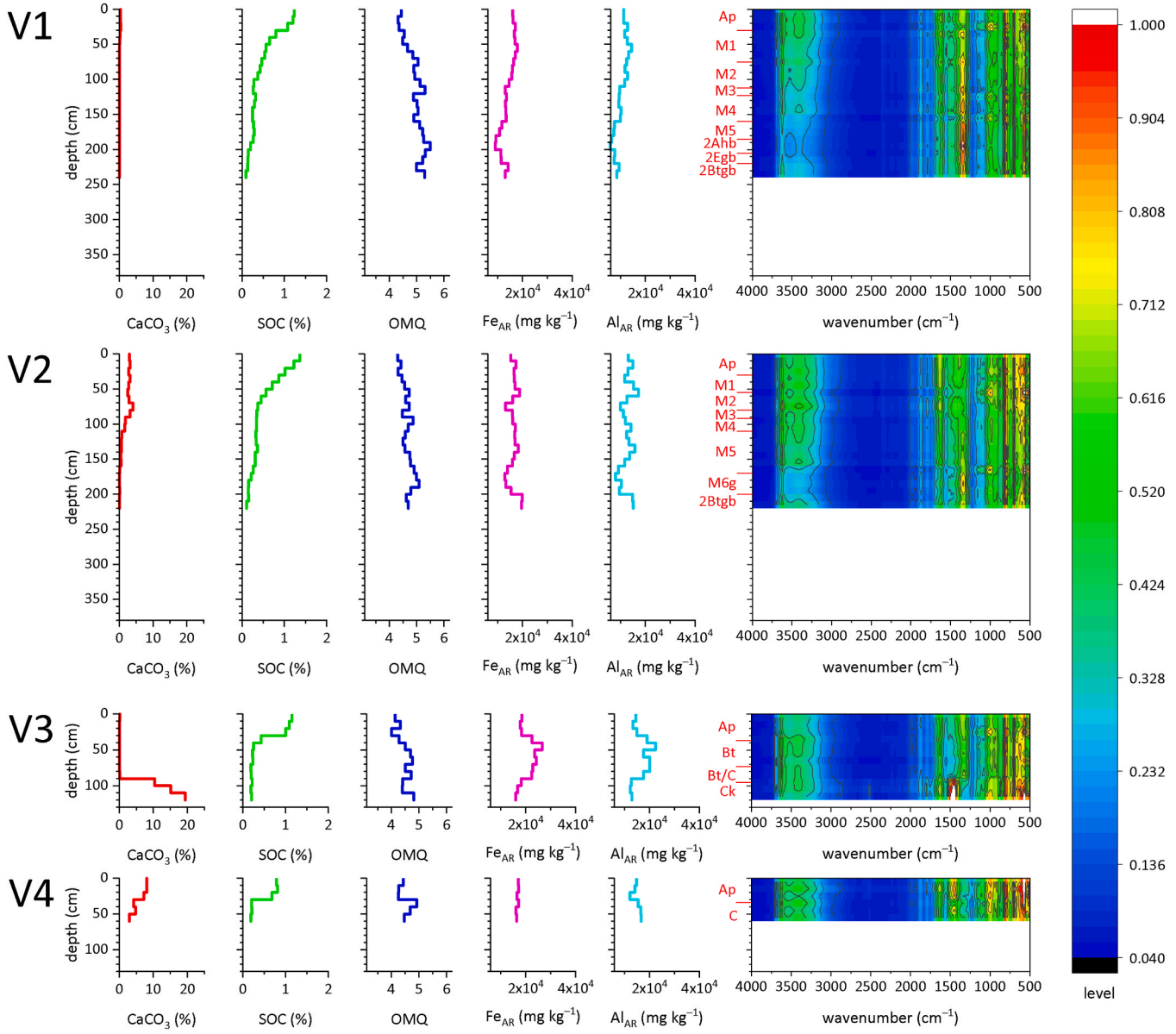

Fig. 5. Vidim – Luvisol region – soil profile distribution of $CaCO_3$, SOC, organic matter quality (OMQ) index, Fe_{AR} and Al_{AR} contents, and spectral maps after spectra normalization by band 810 cm^{-1}.

sediments document significant truncation of source Luvisols and admixture of exposed loess (Loba et al., 2023). Carbonates contents below 5 % are no longer reflected in the area 2550–2500 cm^{-1} of spectral maps.

The content of SOC continuously decreases with depth in V1 and V2 profile. It is documented in decreasing 1640 cm^{-1} band intensity in their spectral maps. A more pronounced change in the SOC content in the V3 and V4 profiles forming a lower boundary of Ap horizon was manifested in this band only in the V4 spectra.

The vibration of the OH group, similarly to Brumovice locality, belongs to organic matter and to (oxy)hydroxides. Even though their affiliation is variable, specific layers can be defined based on them in spectral maps. In the case of V1 profile, Ap horizon with higher SOC content and 2Ahb horizon with low SOC, Fe_{AR} and Al_{AR} contents are identifiable. Similar situation (as in 2Ahb) is in M6g layer of V2 profile. In the V3 profile, effect of mineral soil phase is dominant and OH groups band is the most intense in horizons Bt and Bt/C with the highest Fe_{AR} and Al_{AR} contents. Higher Fe_{AR} and Al_{AR} contents are reflected in two narrow peaks (3690 and 3620 cm^{-1}) belonging to vibration of clays (alumosilicates) and Fe oxides (Madejová, 2003; Le Guillou et al., 2015; Tinti et al., 2015). It is their narrowness and the resolution of the spectral map that limits their applicability in identifying individual layers.

Organic matter quality is comparable with Chernozem region. OMQ index varies between 4 and 5.5. The lowest values well indicate Ap horizon in all four profiles. Recent soil management and fresh organic material impute is documented by higher organic matter content with a higher proportion of aliphatic functional groups, which can be found in polysaccharides, proteins, aliphatic organic acids, etc. In the deeper parts of soil profiles, where SOC content is low, OMQ reach the highest values. It could be similarly as in Chernozem region caused by the firm binding of organic matter to the mineral component of the soil and its maturity and resistance to decomposition, which is influenced by the hydrophobicity of its aromatic components (Leue et al., 2010; Maryganova et al., 2010; Bi et al., 2013; Angst et al., 2021). In the case of V1 profile, the high OMQ values appertain to 2Ahb horizon, in V2 profile to M6g respectively. Obvious quality change is documented in V3 and V4 profile at the lower boundary of Ap horizon.

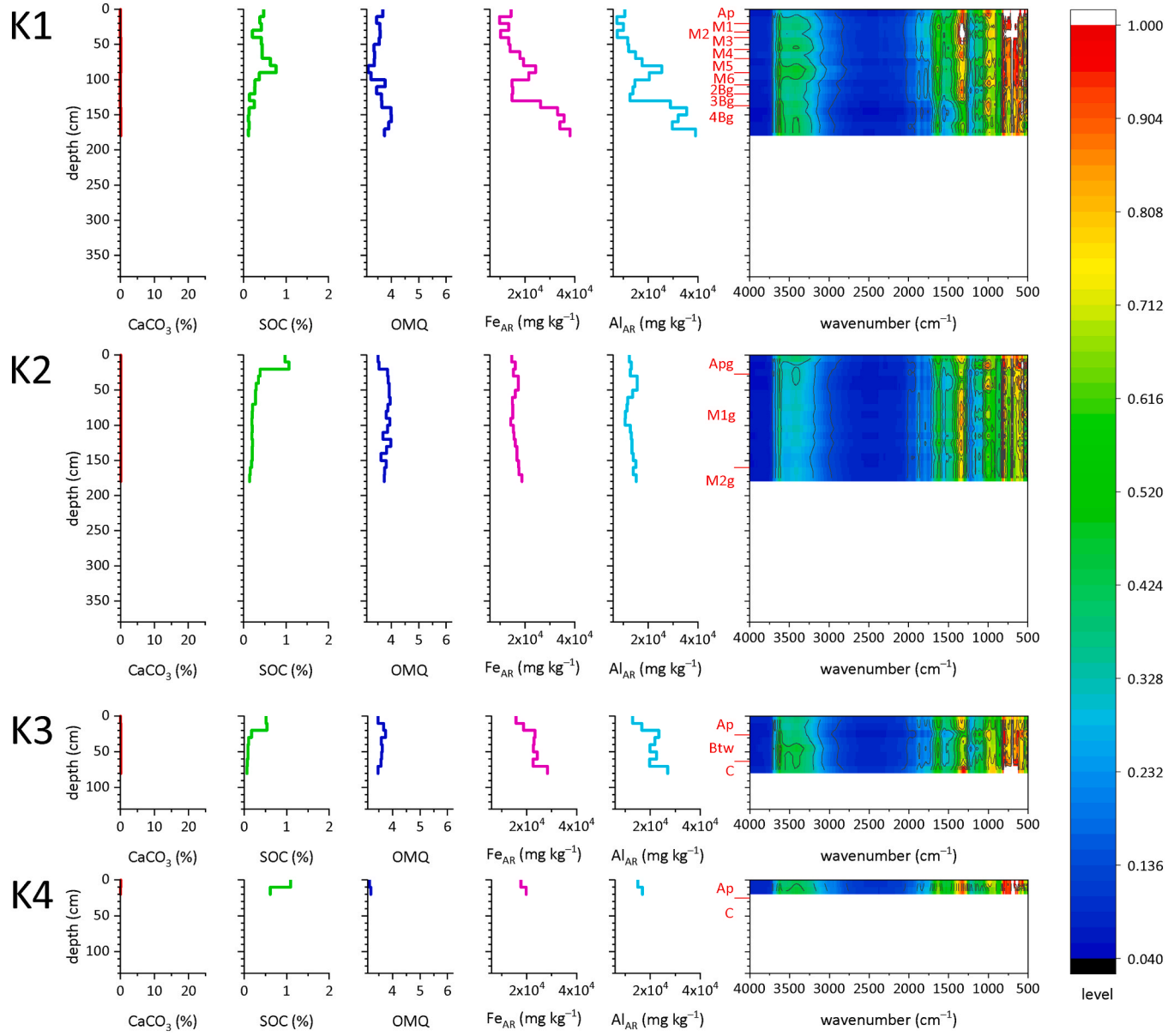

Fig. 6. Kosova hora – Cambisol region – soil profile distribution of $CaCO_3$, SOC, organic matter quality (OMQ) index, Fe_{AR} and Al_{AR} contents, and spectral maps after spectra normalization by band 810 cm^{-1}.
Soil horizons description id adopted from Zádorová et al. (2023).

Soils of Kosova Hora area are characterized by very low or no carbonate content. They contain a tiny amount of organic matter in the soil profile. In the K1 profile, maximal SOC content (0.76 %) was identified in a depth of 90 cm, while it peaks in topsoil of K2, K3 and K4 profiles. While maintaining the same scale as for Chernozems and Luvisols, only a few differences between the individual layers can be seen in the spectral maps. Bands of iron oxides and aluminosilicates (3690 and 3620 cm^{-1}) are more prominent here, which corresponds to the character of Cambisols given by their pedogenesis. Transformation of parent material should be evident from the formation of soil structure, mostly brownish coloration and increasing clay percentage. Cambic horizons also usually show higher oxide and/or clay contents than the underlying layer (IUSS Working Group WRB, 2022). In the locality, however, the situation is complicated by the mixing of other materials, mainly loess-like silty sediment and clayey material, into the granodiorite eluvium. In addition to significant weathering, the micromorphological record also revealed relatively well-developed clay coatings in Btw horizon (K3) and 4Bg (K1), not very typical for this area, representing a transition from Cambisols to Luvisols (Zádorová et al., 2023). This is consistent with the higher content of aluminosilicates and iron oxides in the Btw horizon (K3), which is also evident from the intensity of the normalized bands 3690 and 3620 cm^{-1}.

The most striking differences can be seen in the wide band of OH groups. A pair of layers M5 and M6 is well identifiable in the K1 soil profile. There are relatively high contents of SOC, Fe_{AR} and Al_{AR}. Zádorová et al. (2023) attributed an increase of different compounds (not only SOC, but also human-bound substances) in M5 layer to the higher precipitation and erosional activity in 1960's and later stabilization of the layer. The deepest layers (3Bg and 4Bg of this profile), dated to Early Holocene, with the highest Fe_{AR} and Al_{AR} contents are also separated from others in this vibration band and their very low SOC content is manifested in low intensity of 1620 cm^{-1} band too. Iron and aluminium contents are relatively constant in K2 profile and that is why the Apg horizon richer in organic matter is clearly visible here in the band of OH groups.

It can be said that the soil organic matter in this region contains a

higher proportion of aliphatic components than the organic matter of Chernozems and Luvisols. OMQ index values varies between 3 and 4. Low values are in Ap horizons of K2 and K4 soil profiles. Interestingly, the organic matter of profile K1 in a depth of 90 cm (M5) has the least aromatic components, whereas the SOC content is the highest. Stability and resistance of organic matter is based on organic matter chemical composition but also (and probably mainly) on organic matter interactions with soil minerals. SOM is stabilized by two mechanisms: by the formation of mineral-associated organic matter and by the formation of aggregates (Angst et al., 2021). Higher proportion of aliphatic groups in the stable soil aggregates was present by Thai et al. (2022). Polysaccharides and proteins as aliphatic components of SOM with affinity to organo-metallic complexes formation was present by Angst et al. (2021). Thus, it is possible that the stabilization (of otherwise relatively mobile organic matter) is caused by binding to iron oxyhydroxides. Positive effect of iron forms on aggregates stability was found by Pavlů et al. (2022) exactly in this region.

4. Conclusions

We showed the possibility of identifying differences among Colluvisols layers using DRIFT spectroscopy. For testing, a specific environment with significant erosional redistribution and complex soil development was used, where sedimentary layers of different ages and in-situ formed soils were combined. The three localities were chosen from three different soil-climatic regions. As the primary aim was to demonstrate the method described above, we didn't attempt to explain in detail the causes of the differences in the individual colluvial layers or to describe the history of their development in a landscape context.

We can conclude that the set of spectral parameters based on normalization using quartz spectral bands and organic matter quality evaluation using the newly designed OMQ index based on the ratio of bands (aliphatic compounds spectral bands (2930 cm^{-1}) and aromatics and C═O groups band around 1640 cm^{-1}) reflectance is a beneficial tool for the description of soil parameters. It is equally suitable for non-carbonate soils as well as for soils with higher carbonate contents, which otherwise usually cause difficulties in the interpretation of SOM spectral parameters. It does not require complicated and time-consuming sample preparation, provides a comprehensive view of the soil and its mineral and organic components, and can provide information that is difficult to measure with other methods. From the perspective of quantifying some soil components, this method does not provide absolutely accurate results. The best results were obtained when predicting the carbonate content in Chernozem and Luvisol regions (R^2 was 0.89 and 0.88, respectively; range of $CaCO_3$ content 0–25 %). The amount of organic carbon was predicted from such normalized spectra with less confidence ($R^2 = 0.64$) because of the relatively low variability of organic carbon content in the studied soils (min = 0.06 %; max = 1.90 %). However, it can be used to define areas or soil horizons with similar parameters and thus limit the number of samples analysed by more precise and sophisticated methods. OMQ is another indicator that helps to identify and describe individual colluvial layers. The highest values of this indicator were found in in the Chernozem region (> 6, while, e.g., in the Cambisol region is < 1), especially in the layers corresponding to the oldest sediments or buried in-situ horizons. This means that there is organic matter with the lowest proportion of aliphatic components, which can be characterised as stable and relatively recalcitrant and very resistant to decomposition. In the Cambisol region, the organic matter contains a higher proportion of aliphatic components than the organic matter of Chernozems and Luvisols. Iron oxyhydroxides contribute to its stabilisation in the soil and the spectral band related to OH groups of these oxyhydroxides has also been used to identify the buried B horizon of the Cambisols.

Finally, infrared spectroscopy is a relatively inexpensive method of analysis, and the aforementioned limitation on the number of samples for more specific analyses can mean a significant reduction in the cost of soil survey.

Declaration of Competing Interest

The authors declare that they have no known competing financial interests or personal relationships that could have appeared to influence the work reported in this paper.

Data Availability

Data will be made available on request.

Acknowledgements

The authors acknowledge the financial support of the project No. 21-11879S of Czech Science Foundation (GACR). We thank the two unknown reviewers for their valuable suggestions.

References

Angst, G., Mueller, K.E., Nierop, K.G.J., Simpson, M.J., 2021. Plant- or microbial-derived? A review on the molecular composition of stabilized soil organic matter. Soil Biol. Biochem. 156, 108189 https://doi.org/10.1016/j.soilbio.2021.108189.

Artz, R.R.E., Chapman, S.J., Campbell, C.D., 2006. Substrate utilisation profiles of microbial communities in peat are depth dependent and correlate with whole soil FTIR profiles. Soil Biol. Biochem. 38, 2958–2962. https://doi.org/10.1016/j.soilbio.2006.04.017.

Barra, I., Haefele, S.M., Sakrabani, R., Kebele, F., 2021. Soil spectroscopy with the use of chemometrics, machine learning and pre-processing techniques in soil diagnosis: recent advancese – a review. Trends Anal. Chem. 135, 116166 https://doi.org/10.1016/j.trac.2020.116166.

Benedet, L., Silva, S.H.G., Mancini, M., Teixeira, A.F.S., Inda, A.V., Demattê, J.A.M., Curi, N., 2022. Variation of properties of two contrasting Oxisols enhanced by pXRF and vis-NIR. J. South Am. Earth Sci. 115, 103748 https://doi.org/10.1016/j.jsames.2022.103748.

Bi, R., Lu, Q., Yuan, T., Zhou, S., Yuan, Y., Cai, Y., 2013. Electrochemical and spectroscopic characteristics of dissolved organic matter in a forest soil profile. Res. J. Environ. Sci. 25, 2093–2101. https://doi.org/10.1016/S1001-0742(12)60283-6.

Boardman, J., Poesen, J., 2006. Soil Erosion in Europe. Wiley, Chichester. https://doi.org/10.1002/0470859202.

Bosch-Reig, F., Gimeno-Adelantado, J.V., Bosch-Mossi, F., Doménech-Carbó, A., 2017. Quantification of minerals from ATR-FTIR spectra with spectral interferences using the MRC method. Spectrochim. Acta Part A: Mol. Biomol. Spectrosc. 181, 7–12. https://doi.org/10.1016/j.saa.2017.02.012.

Brady, N.C., Weil, R.R., 2008. The Nature and Properties of Soils. Pearson Prentice Hall, Saddle River.

Chaopricha, N.T., Marín-Spiotta, E., 2014. Soil burial contributes to deep soil organic carbon storage. Soil Biol. Biochem. 69, 251–264. https://doi.org/10.1016/j.soilbio.2013.11.011.

Chlupáč, I., Brzobohatý, R., Kovanda, J., Straník, Z., 2002. Geologická minulost České republiky (in Czech). Academia, Praha.

Clemens, G., Stahr, K., 1994. Present and past soil erosion rates in catchments of the Kraichgau area (SW-Germany. Catena 22, 153–168. https://doi.org/10.1016/0341-8162(94)90023-X.

Cools N., De Vos B., 2016. Part X: Sampling and analysis of soil. Page 29 + Annex in Centre UIFPC, editor. Manual on methods and criteria for harmonized sampling, assessment, monitoring and analysis of the effects of air pollution on forests. Thünen Institute of Forest Ecosystems, Eberswalde.

Cunha, T.J.F., Novotny, E.H., Madari, B.E., Martin-Neto, L., De, O., Rezende, M.O., Canelas, L.P., De, M., Benites, V., 2009. Spectroscopy characterization of humic acids isolated from Amazonian Dark Earth Soils (Terra Preta de Índio). In: Woods, W.I., Teixeira, W.G., Lehman, J., Steiner, C., Winklerprins, A., Rebellato, L. (Eds.), Amazonian Dark Earths: Wim Sombroek's Vision. Springer, Berlin, pp. 363–372.

Dotterweich, M., 2008. The history of soil erosion and fluvial deposits in small catchments of Central Europe: deciphering the long-term interaction between humans and the environment – a review. Geomorphology 101, 192–208. https://doi.org/10.1016/j.geomorph.2008.05.023.

Ellerbrock, R.H., Gerke, H.H., Bachmann, J., Goebel, M.-O., 2005. Composition of organic matter fractions for explaining wettability of three forest soils. Soil Sci. Soc. Am. J. 69, 57–66. https://doi.org/10.2136/sssaj2005.0057.

Foucher, A., Salvador-Blanes, S., Evrard, O., Simonneau, A., Chapron, E., Courp, T., Cerdan, I., Adriaensen, H., Lecompte, F., Desmet, M., 2014. Increase in soil erosion after agricultural intensification: evidence from a lowland basin in France. Anthropocene 7, 30–41. https://doi.org/10.1016/j.ancene.2015.02.001.

Fuchs, M., Lang, A., 2009. Luminescence dating of hillslope deposits – a review. Geomorphology 109, 17–26. https://doi.org/10.1016/j.geomorph.2008.08.025.

Gerzabek, M.H., Antil, R.S., Kögel-Knabner, I., Knicker, H., Kirchmann, H., Haberhauer, G., 2006. How are soil use and management reflected by soil organic matter characteristics: a spectroscopic approach. Eur. J. Soil Sci. 57, 485–494. https://doi.org/10.1111/j.1365-2389.2006.00794.x.

Gozukara, G., Acar, M., Ozlu, E., Dengiz, O., Hartemink, A.E., Zhang, Y., 2022. A soil quality index using Vis-NIR and pXRF spectra of a soil profile. Catena 211, 105954. https://doi.org/10.1016/j.catena.2021.105954.

Haberhauer, G., Rafferty, B., Strebl, F., Gerzabek, M.H., 1998. Comparison of the composition of forest soil litter derived from three different sites at various decompositional stages using FTIR spectroscopy. Geoderma 83, 331–342. https://doi.org/10.1016/S0016-7061(98)00008-1.

Hahn, A., Vogel, H., Andó, S., Garzanti, E., Kuhn, G., Lantzsch, H., Schüürman, J., Vogt, Ch, Zabel, M., 2018. Using Fourier transform infrared spectroscopy to determine mineral phases in sediments. Sediment. Geol. 375, 27–35. https://doi.org/10.1016/j.sedgeo.2018.03.010.

Henkner, J., Ahlrichs, J.J., Downey, S., Fuchs, M., James, B.R., Junge, A., Knopf, T., Scholten, T., Kühn, P., 2018. Archaeopedological analysis of colluvial deposits in favourable and unfavourable areas: reconstruction of land use dynamics in SW Germany. R. Soc. Open Sci. 5, 171624 https://doi.org/10.1098/rsos.171624.

IUSS Working Group WRB, 2022. World Reference Base for Soil Resources 2022. International Soil Classification System for Naming Soils and Creating Legends for Soil Maps. FAO, Rome.

Jakšík, O., Kodešová, R., Kubiš, A., Stehlíková, I., Drábek, O., Kapička, A., 2015. Soil aggregate stability within morphologically diverse areas. Catena 127, 287–299. https://doi.org/10.1016/j.catena.2015.01.010.

Jalal, F.E., Xu, Y., Iqbal, M., Javed, M.F., Jamhiri, B., 2021. Predictive modelling of swell-strength of expansive soils using artificial intelligence approaches: ANN, ANFIS and GEP. J. Environ. Manag. 289, 112420 https://doi.org/10.1016/j.jenvman.2021.112420.

Kaiser, K., Schneider, T., Küster, M., Dietze, E., Fülling, A., Heinrich, S., Kappler, C., Nelle, O., Schult, M., Theuerkauf, M., Vogel, S., Maartje de Boer, A., Börner, A., Preusser, F., Schwabe, M., Ulrich, J., Wirner, M., Bens, O., 2020. Palaeosols and their cover sediments of a glacial landscape in northern central Europe: Spatial distribution, pedostratigraphy and evidence on landscape evolution. Catena 193, 104647. https://doi.org/10.1016/j.catena.2020.104647.

Kappler, C., Kaiser, K., Tanski, B., Klos, F., Fülling, A., Mrotzek, A., Sommer, M., Bens, O., 2018. Stratigraphy and age of colluvial deposits indicating Late Holocene soil erosion in northeastern Germany. Catena 170, 224–245. https://doi.org/10.1016/j.catena.2018.06.010.

Keesstra, S., Pereira, P., Novara, A., Brevik, E.C., Azorin-Molina, C., Parras-Alcántara, L., Jordán, A., Cerdà, A., 2016. Effects of soil management techniques on soil water erosion in apricot orchards. Sci. Total Environ. 551–552, 357–366. https://doi.org/10.1016/j.scitotenv.2016.01.182.

Kincl, D., Formánek, P., Vopravil, J., Nerušil, P., Menšík, L., Janků, J., 2022. Soil-conservation effect of intercrops in silage maize. Soil Water Res. 17, 180–190. https://doi.org/10.17221/36/2022-SWR.

Kołodyńska-Gawrysiak, R., Poesen, J., Gawrysiak, L., 2018. Assessment of long-term Holocene soil erosion rates in Polish loess areas using sedimentary archives from closed depressions. Earth Surf. Process. Landf. 43, 978–1000. https://doi.org/10.1002/esp.4296.

Kühn, P., Lehndorff, E., Fuchs, M., 2017. Lateglacial to Holocene pedogenesis and formation of colluvial deposits in a loess landscape of Central Europe (Wetterau, Germany). Catena 154, 118–135. https://doi.org/10.1016/j.catena.2017.02.015.

Le Guillou, F., Wetterlind, W., Viscarra Rossel, R.A., Hicks, W., Grundy, M., Tuomi, S., 2015. How does grinding affect the mid-infrared spectra of soil and their multivariate calibrations to texture and organic carbon? Soil Tillage Res. 53 (8), 913–921. https://doi.org/10.1071/SR15019.

Leue, M., Ellerbrock, R.H., Gerke, H.H., 2010. DRIFT mapping of organic matter composition at intact soil aggregate surfaces. Vadose Zone J. 9, 317–324. https://doi.org/10.2136/vzj2009.0101.

Loba, A., Waroszewski, J., Sykuła, M., Kabala, C., Egli, M., 2022. Meteoric 10Be, 137Cs and 239+240Pu as tracers of long- and medium-term soil erosion—a review. Minerals 12, 359. https://doi.org/10.3390/min12030359.

Loba, A., Zhang, J., Tsukamoto, S., Kasprzak, M., Kowalska, J.B., Frechen, M., Waroszewski, J., 2023. Multiproxy approach to the reconstruction of soil denudation events and the disappearance of Luvisols in the loess landscape of south-western Poland. Catena 220, 106724. https://doi.org/10.1016/j.catena.2022.106724.

Madejová, J., 2003. FTIR techniques in clay mineral studies. Vib. Spectrosc. 31, 1–10. https://doi.org/10.1016/S0924-2031(02)00065-6.

Margenot, A.J., Calderón, F.J., Bowles, T.M., Parikh, S.J., Jackson, L.E., 2015. Soil organic matter functional group composition in relation to organic carbon, nitrogen, and phosphorus fractions in organically managed tomato fields. Soil Sci. Soc. Am. J. 79, 772–782. https://doi.org/10.2136/sssaj2015.02.0070.

Maryganova, V., Szajdak, L.W., Tychinskaya, L., 2010. Hydrophobic and hydrophilic properties of humic acids from soils under shelterbelts of different ages. Chem. Ecol. 26 (2), 25–33. https://doi.org/10.1080/02757540.2010.501138.

Matamala, R., Calderón, F.J., Jastrow, J.D., Fan, Z., Hofmann, S.M., Michaelson, G., Mishra, U., Ping, Ch, 2017. Influence of site and soil properties on the DRIFT spectra of northern cold region soils. Geoderma 305, 80–91. https://doi.org/10.1016/j.geoderma.2017.05.014.

Minasny, B., McBratney, A.B., 2008. Regression rules as a tool for predicting soil properties from infrared reflectance spectroscopy. Chemom. Intell. Lab. Syst. 94, 72–79. https://doi.org/10.1016/j.chemolab.2008.06.003.

Ng, W., Minasny, B., Montazerolghaem, M., Padarian, J., Ferguson, R., Bailey, S., McBratney, A.B., 2019. Convolutional neural network for simultaneous prediction of several soil properties using visible/near-infrared, mid-infrared, and their combined spectra. Geoderma 352, 251–267. https://doi.org/10.1016/j.geoderma.2019.06.016.

Pärnpuu, S., Astover, A., Tõnutare, T., Penu, P., Kauer, K., 2022. Soil organic matter qualification with FTIR spectroscopy under different soil types in Estonia. Geoderma Reg. 28, e00483 https://doi.org/10.1016/j.geodrs.2022.e00483.

Pavlů, L., Kodešová, R., Vašát, R., Fér, M., Klement, A., Nikodem, A., Kapička, A., 2022. Estimation of the stability of topsoil aggregates in areas affected by water erosion using selected soil and terrain properties. Soil . Res. 219, 105348 https://doi.org/10.1016/j.still.2022.105348.

Penížek, V., Zádorová, T., Kodešová, R., Vaněk, A., 2016. Influence of elevation data resolution on spatial prediction of colluvial soils in a luvisol region. PLoS One 11 (11), 165699. https://doi.org/10.1371/journal.pone.0165699.

Poręba, G., Śnieszko, Z., Moska, P., 2015. Application of OSL dating and 137Cs measurements to reconstruct the history of water erosion: a case study of a Holocene colluvium in Świerklany, south Poland. Quat. Int. 374, 187–197. https://doi.org/10.1016/j.quaint.2015.04.004.

Poręba, G., Śnieszko, Z., Moska, P., Mroczek, P., Malik, I., 2019. Interpretation of soil erosion in a Polish loess area using OSL, 137Cs, 210Pbex, dendrochronology and micromorphology — case study: Biedrzykowice site (S Poland). Geochronometria 46, 57–78. https://doi.org/10.1515/geochr-2015-0109.

Sagová-Marečková, M., Zádorová, T., Penížek, V., Omelka, M., Tejnecký, V., Průchová, P., Chuman, T., Drábek, O., Burešová, A., Vaněk, A., Kopecký, J., 2016. The structure of bacterial communities along two vertical profiles of a deep colluvial soil. Soil Biol. Biochem. 101, 65–73. https://doi.org/10.1016/j.soilbio.2016.06.026.

Sarapatka, B., Cap, L., Bila, P., 2018. The varying effect of water erosion on chemical and biochemical soil properties in different parts of Chernozem slopes. Geoderma 314, 20–26. https://doi.org/10.1016/j.geoderma.2017.10.037.

Scherer, S., Deckers, K., Dietel, J., Fuchs, M., Henkner, J., Höpfer, B., Junge, A., Kandeler, E., Lehndorff, E., Leinweber, P., Lomax, J., Miera, J., Poll, C., Toffolo, M. B., Knopf, T., Scholten, T., Kühn, P., 2021a. What's in a colluvial deposit? Perspectives from archaeopedology. Catena 198, 105040. https://doi.org/10.1016/j.catena.2020.105040.

Scherer, S., Höpfer, B., Deckers, K., Fischer, E., Fuchs, M., Kandeler, E., Lechterbeck, J., Lehndorff, E., Lomax, J., Marhan, S., Marinova, E., Meister, J., Poll, C., Rahimova, H., Rösch, M., Wroth, K., Zastrow, J., Knopf, T., Scholten, T., Kühn, P., 2021b. Middle Bronze Age land use practices in the northwestern Alpine foreland – a multi-proxy study of colluvial deposits, archaeological features and peat bogs. SOIL 7, 269–304. https://doi.org/10.5194/soil-7-269-2021.

Senthil Kumar, R., Rajkumar, P., 2014. Characterization of minerals in air dust particles in the state of Tamilnadu, India through FTIR, XRD and SEM analyses. Infrared Phys. Technol. 67, 30–41. https://doi.org/10.1016/j.infrared.2014.06.002.

Skjemstad, J.O., Baldock, J.A., 2007. Total and organic carbon. In: Carter, M.R., Gregorich, E.G. (Eds.), Soil Sampling and Methods of Analysis. CRC Press, Boca Raton.

Sklenička, P., Šímová, P., Hrdinová, K., Šálek, M., 2014. Changing rural landscapes along the border of Austria and the Czech Republic between 1952 and 2009: Roles of political, socioeconomic and environmental factors. Appl. Geogr. 47, 89–98. https://doi.org/10.1016/j.apgeog.2013.12.006.

Stockmann, U., Cattle, S.R., Minasny, B., McBratney, A.B., 2016. Utilizing portable X-ray fluorescence spectrometry for in-field investigation of pedogenesis. Catena 139, 220–231. https://doi.org/10.1016/j.catena.2016.01.007.

Stuart, B.H., 2004. Infrared Spectroscopy: Fundamentals and Applications. Wiley, New Jersey.

Thai, S., Pavlů, L., Tejnecký, V., Vokurková, V., Nozari, S., Borůvka, L., 2021. Comparison of soil organic matter composition under different land uses by DRIFT spectroscopy. Plant Soil Environ. 67 (5), 255–263. https://doi.org/10.17221/11/2021-PSE.

Thai, S., Davídek, T., Pavlů, L., 2022. Causes clarification of the soil aggregates stability on mulched soil. Soil Water Res. 17, 91–99. https://doi.org/10.17221/151/2021-swr.

Tinti, A., Tugnoli, V., Bonora, S., Francioso, O., 2015. Recent applications of vibrational mid-Infrared (IR) spectroscopy for studying soil components: a review. J. Cent. Eur. Agric. 16 (1), 1–22. https://doi.org/10.5513/JCEA01/16.1.1535.

Vagenas, N.V., Gatsouli, A., Kontoyannis, C.G., 2003. Quantitative analysis of synthetic calcium carbonate polymorphs using FT-IR spectroscopy. Talanta 59, 831–836. https://doi.org/10.1016/S0039-9140(02)00638-0.

Van Oost, K., Govers, G., De Alba, S., Quine, T.A., 2006. Tillage erosion: a review of controlling factors and implications for soil quality. Prog. Phys. Geogr. 30, 443–466. https://doi.org/10.1191/0309133306pp487ra.

Veum, K.S., Goyne, K.W., Kremer, R.J., Miles, R.J., Sudduth, K.A., 2014. Biological indicators of soil quality and soil organic matter characteristics in an agricultural management continuum. Biogeochemistry 117, 81–99. https://doi.org/10.1007/s.

Williams, P.C., Sobering, D.C., 1993. Comparison of commercial near infrared transmittance and reflectance instruments for analysis of whole grains and seeds. J. Infrared Spectrosc. 1 (1), 25–32. https://doi.org/10.1255/jnirs.3.

Zádorová, T., Penížek, V., 2018. Formation, morphology and classification of colluvial soils: a review. Eur. J. Soil Sci. 69, 577–591. https://doi.org/10.1111/ejss.12673.

Zádorová, T., Penížek, V., Šefrna, L., Drábek, O., Mihaljevič, M., Volf, Š., Chuman, T., 2013. Identification of Neolithic to Modern erosion–sedimentation phases using geochemical approach in a loess covered sub-catchment of South Moravia, Czech Republic. Geoderma 195–196, 56–69. https://doi.org/10.1016/j.geoderma.2012.11.012.

Zádorová, T., Žížala, D., Penížek, V., Čejková, Š., 2014. Relating extent of colluvial soils to topographic derivatives and soil variables in a Luvisol sub-catchment, Central Bohemia, Czech Republic. Soil Water Res. 9, 47–57. https://doi.org/10.17221/57/2013-SWR.

Zádorová, T., Penížek, V., Vašát, R., Žížala, D., Chuman, T., Vaněk, A., 2015. Colluvial soils as a soil organic carbon pool in different soil regions. Geoderma 253–254, 122–134. https://doi.org/10.1016/j.geoderma.2015.04.012.

Zádorová, T., Penížek, V., Lisá, L., Koubová, M., Žížala, D., Tejnecký, V., Drábek, O., Kodešová, R., Fér, M., Klement, A., Nikodem, A., Vokurková, P., Pavlů, L., Vaněk, A., Moska, P., 2023. Formation of Colluvisols in different soil regions and slope positions (Czechia): Stratification and upbuilding of colluvial profiles. Catena 221, 106755. https://doi.org/10.1016/j.catena.2022.106755.